Weighted Iterative List-Mode Reconstruction for the High Resolution Research Tomograph

A. Rahmim[1], M. Lenox[2], A. J. Reader[3], C. Michel[2], Z. Burbar[2], T. J. Ruth[4], and V. Sossi[1]
[1]Department of Physics and Astronomy, University of British Columbia, Vancouver, BC Canada
[2]CTI Inc., Knoxville, TN USA
[3]Department of Instrumentation and Analytical Science UMIST, Manchester, UK
[4]UBC/Triumf, Vancouver, BC Canada

***Abstract*— An attenuation/normalization weighted iterative list-mode reconstruction algorithm with random events correction was developed and implemented for the depth-encoding high resolution research tomograph. The final goal is to compare frame-mode versus list-mode reconstructions including all corrections to address time-cost for a specified image quality. As a first step, we have checked that list-mode reconstructed images are comparable statistically with images generated by 3D-OSEM for a wide range of random coincidences. List-mode reconstruction was also parallelized successfully on a Linux cluster.**

I. Introduction

In 3D positron emission tomography (PET) systems, there is a continuous effort to increase sensitivity and to improve spatial resolution. This, in turn, brings about the need for different approaches to data collection and image reconstruction in order to make use of the high sampling capabilities of such systems. Conventional tomographs inherently bin the collected data into histogram bins. In the case of high resolution tomographs with list-mode acquisition capability, such as the new high resolution research tomograph (HRRT), it is worthwhile investigating the applicability of iterative list-mode reconstruction schemes. The motivation is two-fold. First, in low-statistics 3D PET scans, list-mode reconstruction is in principle able to be performed more quickly and efficiently than 3D-OSEM: when the reconstruction of short time frames is required, the number of events acquired may be in-fact less than the number of lines of response (LORs) in a full sinogram set. Second, when histogram based reconstruction methods are used, data are often compressed (axially or radially) to reduce the data set size[1]. This has been shown to adversely affect axial/transaxial resolution of images reconstructed using 3D-OSEM, especially as one moves away from the center of the field-of-view (FOV) [1]. In the case of list-mode reconstruction, since events are considered one-be-one, histogram data compression is in principle not needed, thus resulting in better image resolution and uniformity at no extra time cost.

II. List-mode Expectation Maximization Reconstruction Algorithm

The list-mode expectation maximization (LM-EM) reconstruction algorithm can be formulated from first principles [2], as well as derived from an expression for the likelihood function for statistically independent, Poisson-distributed histogram data, where the sum over histogram bins is converted to a summation over events [3]. Denoting λ_j^m as the image intensity in voxel j (j=1...J) at the mth iteration, and p_{ij} as the probability of an emission from voxel j being detected along LOR i (often referred to as the "system matrix"), the resulting LM-EM algorithm is given by

$$\lambda_j^{m+1} = \frac{\lambda_j^m}{\sum_{i=1}^{I} p_{ij}} \sum_{k=1}^{N} p_{i_k j} \frac{1}{\sum_{b=1}^{J} p_{i_k b} \lambda_b^m} \qquad (1)$$

where i_k refers to the LOR along which the kth list-mode event is detected and N is the number of measured events. The sensitivity factor $\sum_{i=1}^{I} p_{ij}$ is a summation over all possible measurable LORs (i=1...I), thus incorporating the informational benefit of all the LORs which could receive counts.

In order to accelerate the LM-EM algorithm, one notes that the approach of Eq. (1) may be extended to a data subsets implementation [4], [5], in which the list-mode data are divided into appropriate *time* subsets. One must note that list-mode subsets exhibit a fundamental difference with histogram-based subsets. This is because each list-mode subset can be thought of as a lower-statistic scan in its own right. This observation may point to another advantage of list-mode reconstruction. It has been shown [6] that the way in which histogram-data subsets are chosen and ordered has an effect on the resulting reconstructions. The requirement of maximum variation between the data subsets is inherently fulfilled with list-mode subsets.

Conventionally, EM algorithms have been applied to measured data pre-corrected by normalization and attenuation measurements. However, similar to histogram-mode reconstruction schemes, normalization and/or attenuation weighting of the LM-EM is possible. Since probability of attenuation for all points along a LOR is independent of the point of origin along the path for PET, the LM-EM algorithm may be properly weighted by simply scaling all elements in a row of the system matrix P=$(p_{ij})_{I\times J}$ by the same factor as calculated by the attenuation and normalization scans. This operation is mathematically equivalent to multiplying P by a

[1]In the case of the HRRT, with no data compression, one has to deal with a histogram size of 1.5G bytes!

diagonal[2] matrix $W=(w_{ii})_{I\times I}$ which allows a weight to be assigned to each LOR, to account for sensitivity variations due to attenuation and normalization. Such matrix factorization results in the emergence of a cancellation in EM algorithms, in general, and for the weighted LM-EM algorithm, in particular:

$$\lambda_j^{m+1} = \frac{\lambda_j^m}{\sum_{i=1}^{I} w_{ii} p_{ij}} \sum_{k=1}^{N} p_{i_k j} \frac{1}{\sum_{b=1}^{J} p_{i_k b} \lambda_b^m} \qquad (2)$$

The cancellation of w_{ii} everywhere, except in the sensitivity factor, which is only calculated once, considerably eases the direct inclusion of normalization and/or attenuation correction in EM algorithms, commonly referred to as weighted schemes. It has been observed [7] that weighted OSEM results in better image quality when compared to the unweighted case, in which the emission scan is simply pre-corrected by normalization/attenuation measurements[3].

In this study we implemented the weighted list-mode expectation maximization (WLM-EM) reconstruction algorithm described by Eq. (2) for the HRRT. Backward and forward projections were performed using the Siddon projection algorithm [9] for *both* 3D-OSEM and LM-EM to allow for direct comparison. We implemented a random correction procedure into the reconstruction algorithm, and we investigated various parallelization schemes for the code. The algorithm was tested with several data sets spanning a wide range of acquired number of counts and count rates, to investigate bias and noise characteristics of the WLM-EM for different data acquisition conditions. In particular, a low statistics, high count rate data set is expected to be very sensitive to a possible random correction induced bias. Images were compared to those obtained using the standard weighted 3D-OSEM (or 3D-WOSEM), 67 ring difference, span 9.

III. METHODS

HRRT: Data were taken on the Cologne HRRT [1]. This scanner has an octagonal design, four detector heads consisting of a double 7.5 mm layer of LSO/LSO, while the remaining four have LSO/GSO crystal layers for a total of 119,808 detector crystals(crystal size 2.1 x 2.1 x 7.5 mm^3). The total number of possible LORs is 4.486×10^9.

Phantom: A 20 cm long, 10 cm radius phantom was used. The phantom had three 5 cm diameter cylindrical inserts: one was solid plastic, one was filled with water (cold insert) and one was filled with a ^{18}F radioactivity concentration of 3.39 μCi/ml (hot insert). The phantom itself was filled with a ^{18}F concentration of 0.622 μCi/ml, yielding a hot insert to background ratio of 5.45. The total amount of radioactivity in the scanner field of view (FOV) at the beginning of the scanning procedure was 4.16 mCi.

[2]This matrix will not be diagonal if one also includes effects of crystal penetration and inter-crystal scattering. Including such effects results in a high reduction in the sparseness of the matrix and increases the computational demand [8].

[3]This can be explained by the fact that in the unweighted scheme, reconstructed images are more sensitive to the noise in normalization/attenuation correction, whereas in weighted OSEM, for each image pixel, only the summation of normalization/attenuation over *all* directions is used.

TABLE I

TABLE OF STATISTICS FOR FRAMES USED IN THE ANALYSIS

Index	Total Activity(mCi)	Trues Rate(kcps)	Random Fraction(%)
1	2.7	814	70.9
2	1.8	718	46.8
3	1.3	425	32.0
4	0.95	208	16.2
5	0.19	69	7.73

Measurements performed: A series of sixteen 20 min long scans was acquired in list-mode, one hour apart. The measurement thus covered 8.7 radioisotope half-lives, yielding a final amount of radioactivity in the FOV of 0.00972 mCi. The subset of the scans listed in table I was used in the analysis presented here. A measured transmission with a ^{137}Cs source was used to correct for attenuation. Detector normalization correction factors were obtained from a 12 hour scan using a rotating rod source. In order to allow a direct comparison with 3D-WOSEM only LORs within a ring difference of 67 were used. For the same reason an axial span of 9 was imposed on the data.

Random correction method: In the case of the HRRT, the ability to use a delayed coincidence time window allows for the measurement of randoms and their storage along with prompts in list-mode acquired data[4]. In frame-mode reconstructions, a random pre-correction method can be utilized, in which the number of trues in each bin is calculated by subtraction of randoms from prompts. In the case of list-mode, however, this is not possible, as the events are read on a time-of-arrival basis. Instead, to address random correction in WLM-EM, we have replaced the number 1 in the numerator of Eq. (2) with -1 upon encountering randoms. For both 3D-WOSEM and WLM-EM, a non-negativity constraint was imposed only when updating image intensities after every subset.

Data analysis: The scans listed in table I were chosen for analysis so as to cover a random fraction (randoms/trues) range between 8% to 71%, which covers most clinically encountered situations. From each acquired data set a low and a high statistics scan were extracted, containing 10M and 80M true counts respectively. Several figures of merit were used in evaluating the reconstruction and random correction methods. A comparison of image axial and radial profiles from non-random corrected data was performed to selectively compare the images obtained from WLM-EM to those obtained with 3D-WOSEM. A similar comparison was performed on the images obtained from random corrected data to investigate the effect of random correction. In addition, an image random fraction (RF = randoms/trues) for each frame and reconstruction algorithm was estimated as: image RF

[4]For systems without a delayed coincidence window, random correction has been previously implemented based on an image-based convolution-subtraction method for linear, non-iterative list-mode reconstruction [10]. Work is currently in progress to incorporate randoms (and scatter) into the system matrix of list-mode EM for such systems [11].

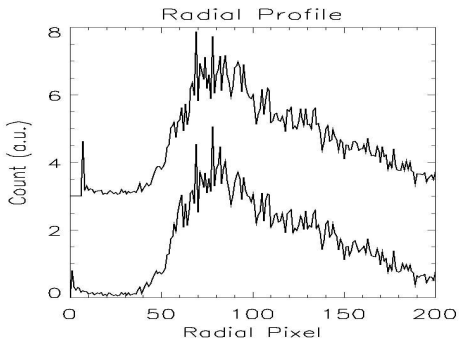

(a) Without random correction

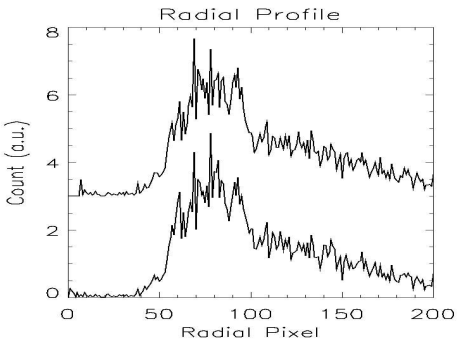

(b) With random correction

Fig. 1. Radial profiles at plane 150 (arbitrarily chosen) of frame 1 (80M true counts) in table I. Images were reconstructed using 3D-WOSEM (higher curve) as well as WLM-EM (lower curve). The 3D-WOSEM profiles have been vertically incremented by 3 units from the origin for better visibility.

= image counts(non-random-corrected)/image counts(random-corrected)-1.

Image RF values are not expected to be numerically equivalent to the random fraction in the acquired data: the true and the random events have a different spatial distribution and will be therefore differently affected by attenuation and sensitivity corrections. However, the ratio between the image RF and the acquired events RF must not vary as a function of acquisition condition if no count rate or number of counts dependent bias is introduced in the data by the random corrections.

Finally, contrast and noise were also estimated following approximately the NEMA NU 2001 protocol. For any given axial plane, the percent contrast Q_H for the hot cylinder was calculated by:

$$Q_H = \frac{C_H/C_B - 1}{A_H/A_B - 1} \times 100\% \quad (3)$$

where C_H and C_B are the average counts in regions of interest (ROIs) placed on the reconstructed images of the hot insert and the background region, respectively, and A_H/A_B is the actual concentration ratio between the two regions (measured to be 5.45). The percentage noise (standard deviation/mean) was calculated by placing eight circular ROIs on different parts of the background image and averaging their values to yield a background mean value and its standard deviation.

Code parallelization: The code parallelization was implemented on the University of British Columbia Dept. of Meteorology Linux Monster Cluster : a 128 x IBM eServers x330 with dual Pentium III: 1 GHz, 1 GB RAM, 256 KB cache system. The message passing interface (MPI) software was utilized to parallelize the WLM-EM reconstruction code. The algorithm essentially consists of having several slave nodes to perform the actual forward and backward projections, results of which are passed to the master node for updating the current image estimate after every subset.

IV. Results

Images reconstructed using WLM-EM and 3D-WOSEM, without random correction, showed excellent agreement in the radial and axial direction. An example is shown in figure 1a where radial profiles for the two algorithms as applied to frame 1 (80M true counts) of table I are shown. Corresponding radial profiles upon the inclusion of random correction are also shown in figure 1b. Similarly, it was found that with the inclusion of random correction, radial and axial profiles were in very good agreement for all images.

TABLE II

TABLE OF RANDOM FRACTIONS

Index	Events RF	Image RF	Image RF/Events RF(%)
1	70.9	52.6	74.1
2	46.8	34.6	73.9
3	32.0	23.4	73.1
4	16.2	11.5	71.0
5	7.73	5.37	69.5

Figure 2 shows contrast vs. noise plots for WLM-EM (with and without random correction) and 3D-WOSEM (with random correction) applied to the five frames shown in table I. Both cases of 10M and 80M true counts are shown in subfigures (a) and (b), respectively. It is observed that random correction for WLM-EM readily improves the contrast vs. noise, and renders WLM-EM results very comparable to corresponding results for random-corrected 3D-WOSEM (within statistical variation).

Image random fractions are shown in table II along with the acquired events random fractions. As can be seen from the table, there is only a very small change in the ratios over a wide range of random fractions. The origin of the small variation will be further investigated.

Parallelization was successfully implemented using MPI for the WLM-EM algorithm. It was found that having the slave nodes directly accessing list-mode data *did* improve the efficiency compared to the case of the master node distributing the actual workload to all the processor. This required multiple read access to a single file as supported by the cluster. An instance of parallelization performance using the scheme

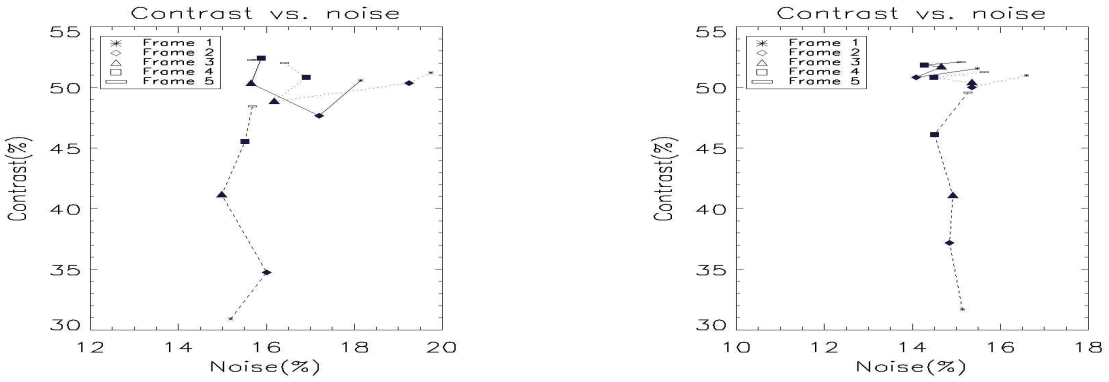

(a) 10M Total Counts

(b) 80M Total Counts

Fig. 2. Contrast vs. noise plots for WLM-EM [without (bottom curve) and with random correction (solid)] as well as 3D-WOSEM (dotted) applied to the five frames in table I. Corresponding WLM-EM and 3D-WOSEM points are within one another's statistical variation (error bars are not shown). Random correction has greater effect for frames with higher random fractions.

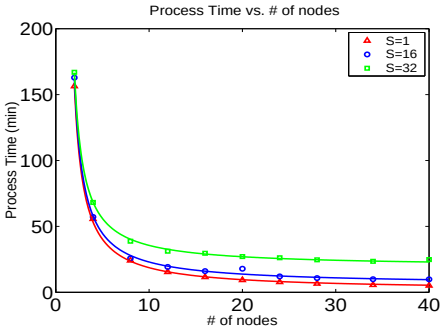

Fig. 3. Process Time (T) vs. number of nodes (N) for a frame with 40M counts is shown. It is readily observed that decreasing the number of subsets increases the efficiency. The points are fit with $T = T_0(\frac{p}{N-1} + (1-p))$, where $N-1$ is the number of slave nodes in MPI and p represents the percentage of reconstruction parallelized.

described is shown in Fig. 3, where a frame with 40M total counts was reconstructed. By direct fitting (as explained in the figure), it was found that by dividing the 40M frame into 1, 8, 16, 32 and 64 subsets, 99%, 98%, 97%, 94% and 88% of the workload were parallelized, respectively.

V. Conclusion

A weighted iterative list-mode reconstruction algorithm with random events correction was developed and implemented for the high resolution research tomograph (HRRT). Preliminary results indicate that list-mode reconstructed images are comparable statistically with images generated by 3D-WOSEM for the HRRT. The algorithm was also parallelized successfully using MPI on a Linux cluster, since 3D-WOSEM is also parallelized on a Linux cluster. Improvements in image quality due to non-compressed data (e.g.minimum span), which in principle introduce no additional time cost for list-mode reconstruction, are currently being evaluated. Furthermore, scatter correction as well as inclusion of a space-variant point resolution function in the system matrix are also currently under study. Once all corrections have been fully implemented, time-cost comparison between frame-mode versus list-mode reconstructions for a specified image quality will be addressed.

References

[1] K. Wienhard, M. Shmand, M. E. Casey, K. Baker, J. Bao, L. Eriksson, W. F. Jones, C. Knoess, M. Lenox, M. Lercher, P. Luk, C. Michel, J. H. Reed, N. Richerzhagen, J. Treffert, S. Vollmar, J. W. Vollmar, J. W. Young, W. D. Heiss, and R. Nutt, "The ECAT HRRT: Performance and First Clinical Application of the New High Resolution Research Tomograph"

[2] L. Parra and H. H. Barrett, "List-mode Likelihood: EM algorithm and image quality estimation demostrated on 2-D PET", *IEEE Trans. Med. Imag.*, vol. 17, no. 2, pp. 228-235, 1998.

[3] R. H. Huesman, G. J. Klein, W. W. Moses, J. Qi, B. W. Reutter and P. R. G. Virador, "List mode maximum likelihood reconstruction applied to positron emission mammography with irregular sampling", *IEEE Trans. Med. Imag.*, vol. 19, pp. 532-537, 2000.

[4] A. J. Reader, K. Erlandsson, M. A. Flower and R. J. Ott, "Fast accurate iterative reconstruction for low-statistics positron volume imaging", *Phys. Med. Biol.*, vol. 43, pp. 835-846, 1998.

[5] A. J. Reader, S. Ally, F. Bakatselos, Roido Manavaki, R. Walledge, A.P. Jeavons, P.J.Julyan, S.Zhao, D. L. Hastings and Jamal Zweit, "One-Pass List-Mode EM Algorithm for High-Resolution 3-D PET Image Reconstruction Into Large Arrays", *IEEE Trans. Nucl. Sci.* vol. 49, pp. 693-699, 2002.

[6] M. Takahashi and K. Ogawa, "Selection of projection set and the order of calculation in ordered subsets expectation maximization method", *IEEE Nucl. Sci. Symp.*, vol. 2, pp. 1408 -1412, 1997.

[7] C. Michel, M. Sibomana, A. Boi, X. Bernard, M. Lonneux, M. Defrise, C. Comtat, P. E. Kinahan and D. W. Townsend, "Preserving Poisson characteristics of PET data with weighted OSEM reconstruction", *IEEE Nucl. Sci. Symp. Conf. Record*, vol. 2, pp. 1323 -1329, 1998.

[8] E. U. Mumcuoglu, R. M. Leahy, S. R. Cherry and E. Hoffman, "Accurate geometric and physical response modelling for statistical image reconstruction in high resolution PET", *IEEE Nucl. Sci. Symp. Conf. Record.*, vol. 3 , pp. 1569-1573, 1996.

[9] R. L. Siddon, "Fast calculation of the exact radiological path for a three-dimensional CT array", *Med. Phys.*, vol, 12, pp. 252-255, 1985.

[10] A. J. Reader, Sha Zhao, P. J. Julyan, D. L. Hastings, J. Zweit, " Adaptive correction of scatter and random events for 3-D backprojected PET data", *IEEE Nucl. Sci. Trans.*, vol. 48, pp. 1350-1356, 2001.

[11] R. Manavaki, A. J. Reader, C. Keller, J. Missimer and R. J. Walledge, "Scatter Modeling for 3-D PET List-Mode EM Reconstruction", *IEEE NSS & MIC 2002 conf. rec.*, Norfolk, VA, Nov 2002.